



Published in final edited form as:

Med Biol Eng Comput. 2012 July ; 50(7): 651–657. doi:10.1007/s11517-012-0899-3.

Is it Possible to Detect Dendrite Currents Using Presently Available Magnetic Resonance Imaging Techniques?

William I. Jay¹, Ranjith S. Wijesinghe¹, Brain D. Dolasinski¹, and Bradley J. Roth²

¹Dept of Physics and Astronomy, Ball State University, Muncie, Indiana

²Dept of Physics, Oakland University, Rochester, Michigan

Abstract

The action currents of a dendrite, peripheral nerve or skeletal muscle create their own magnetic field. Many investigators have attempted to detect neural and dendritic currents directly using magnetic resonance imaging that can cause the phase of the spins to change. Our goal in this paper is to use the calculated magnetic field of a dendrite to estimate the resulting phase shift in the magnetic resonance signal. The field produced by a dense collection of simultaneously active dendrites may be just detectable under the most ideal circumstances, but in almost every realistic case the field cannot be detected using current MRI technology.

Keywords

MRI; action currents; phase shift; dendrite; brain

Introduction

Many researchers have tried to record neural currents using magnetic resonance imaging (MRI) [3, 6, 11, 13, 14, 21, 26]. Such a measurement of action currents would be significant, because it would allow functional imaging of neural activity using the high spatial resolution of MRI and avoid an ill-posed inverse problem to determine the current sources. Functional MRI detects brain activity by measuring the blood oxygenation level-dependent (BOLD) signal [20]. Unfortunately, BOLD measures perfusion rather than neural activity directly. Measurement of the magnetic field of neural currents would better follow the distribution of neural activity in time and space. However, the feasibility of detecting neuronal currents by utilizing MRI is a topic that is still under debate [16, 36]. Neuronal mapping with MRI would provide a noninvasive procedure for mapping the active neural pathways in the brain [18]. Different thought processes, motor responses, sensory responses, language, spatial referencing, and cognition to name a few, could be spatially located within the cortical sections of the cerebrum. The spatial localization would provide a greater understanding of cortex functionality. The direct imaging of the functionality of gray matter sections of the cerebrum depends solely on the magnetic field due to neuronal currents. Neuronal currents stem from the soma, which are chemically transmitted across the synaptic cleft. The propagation of a neural signal through the dendrites and the axons can be represented by multiple current dipoles inside a voxel [15, 16]. The propagating magnetic field then would interact with the already present magnetic field produced across the voxel due to the MRI imaging sequence. The depolarization and re-polarization states would affect the MRI by

Address correspondence to Ranjith S. Wijesinghe, Dept of Physics and Astronomy, Ball State University, Muncie, IN 47306. rswijesinghe@bsu.edu.

adding additional phase contributions to the present precessional states, causing a positive or negative shift in the signal magnitude.

Previously MRI researchers have attempted to calculate the magnetic field associated with action currents [6, 21]. Also, there are many papers in the biomagnetic literature in which magnetic fields of nerves, muscles, and even single axons were calculated numerically [25, 28, 35] or measured using ferrite-core, wire-wound toroids [9, 10, 23, 27, 29, 30, 32–34]. Many investigations have shown results obtained from water phantoms, humans, bloodless turtle brains, rat brains, and theoretical calculations [2, 4, 6, 17]. Some of them have claimed that neuronal magnetic fields caused by neuronal currents can produce measurably large voxel MRI phase and signal changes in the human brain [3, 22, 36]. Others have claimed that the resultant field intensity measured from the human brain is too weak to detect a favorable phase and signal response with MRI [8, 36]. Our goal in this paper is to use calculated magnetic signals of dendritic currents to estimate the changes in MRI signal.

Methods

The magnetic field, \mathbf{B} , emanating from a current distribution can be calculated using the Biot-Savart law:

$$\vec{B} = \int \frac{\mu}{4\pi} \frac{I d\vec{l} \times \vec{r}}{r^3} \quad (1)$$

where μ is the magnetic permeability of free space (we ignore small variations of the permeability within tissue because of its diamagnetic properties), \mathbf{r} is the position vector, and $d\vec{l}$ is the differential length element. This general equation may be applied to the specific cases of axons or dendrites. In a long axon, both depolarization and repolarization phases of the propagating action potential are present simultaneously, at different locations along the fiber, resulting in two oppositely directed dipoles. However, in smaller dendrites only depolarization or repolarization is present at one time. Therefore, we adopt the common practice of representing a dendritic source as a single current dipole [19]. Application of the Biot-Savart law gives:

$$\vec{B} = \frac{\mu}{4\pi} \frac{\vec{p} \times \vec{R}}{R^3} \quad (2)$$

where \mathbf{p} is the current dipole, \mathbf{R} is the vector from the dipole at the source point \mathbf{r}' to the field point \mathbf{r} . In the case of MRI, one is interested in only one component of the magnetic field. Without loss of generality, we choose this to be the z-component. For simplicity, the field point is taken to be in the plane $z'=0$. This gives the following expression for the z-component of the magnetic field:

$$B_z = \frac{\mu}{4\pi} \frac{(-p_x y' + p_y x')}{\sqrt{(x - x')^2 + (y - y')^2 + (z - z')^2}} \quad (3)$$

The resultant field from an ensemble of dendrites will then be the sum of the individual fields given by Eq. (3). This resultant field, a product of neural activity, will make a contribution to the additional phase of the magnetic moments, which MRI detects [22]. Prediction and identification of this phase shift is necessary for the recognition of brain activity in dendrites. The phase contribution ϕ due to the neuronal magnetic field at a given point (x, y, z) in the activated region in a voxel/volume can be calculated using the following equation [36]:

$$\varphi(x, y, z) = \int_0^{TE} \gamma \cdot B_z(x, y, z, t) dt \quad (4)$$

where TE represents the time of the echo sequence and gamma, γ , is the gyromagnetic ratio of the proton ($2.7 \times 10^8 \text{ s}^{-1}\text{T}^{-1}$) [31]. Bodurka and Bandettini [3] have measured the minimum detectable phase shift in an MRI experiment, using a phantom consisting of current-carrying wires in a saline bath. They found that a minimum detectable phase shift of about 0.1° , or 0.0017 radians. For many reasons, reviewed in the discussion, we believe that this value is optimistic, and the actual minimum detectable phase shift is considerably larger. However, in this paper we will adopt 0.0017 radians as the threshold for detectability.

This model represents dendrites in an active voxel of neuronal tissue as dipoles on a variable lattice structure. Dendrite strength, spacing, and orientation are input parameters. Since our goal was to get an upper bound on possible magnitudes of the magnetic fields and associated phase shifts, several of our calculations consider the effects of dipoles arranged uniformly in the voxel, all pointing the x-direction. Clearly, this arrangement is a crude approximation of the complex dendritic arborization present in actual neuronal tissue in the brain. However, this arrangement of dipoles helps us to evaluate the maximum magnetic field created by an active voxel. We also consider several cases in which the dipoles are oriented randomly.

The empirical value for dendrite density is on the order of $10^6 / \text{mm}^3$, and our simulations consider the effects of this density as well as several others [19]. Dendrites range greatly in length from around $300 \mu\text{m}$ for an apical dendrite down to around $10 \mu\text{m}$ for the shortest branching dendrites, and a given tissue volume will often have a larger number of the shorter dendrites [13]. As such, this model assumes all dendrites to have an average length of $L = 30 \mu\text{m}$. Assuming that each active dendrite has an intracellular current of $\mathbf{I} = 1 \text{ nA}$ [6, 22] this gives an equivalent current dipole for a dendrite:

$$\vec{p} = \vec{I} \cdot L = 3 \times 10^{-5} \text{ nAm} \quad (5)$$

An actual voxel of human brain tissue contains overwhelmingly complex neuronal geometries that provide significant difficulties for researchers modeling the brain. Past studies have largely sidestepped this challenge by modeling large-scale tissue volumes or even the whole brain itself using several dipoles. Although this has not been unfruitful, new findings may result from considering more a realistic simulation of the tissue, and our model takes this approach.

Our mathematical model has the capability to simulate the field resulting from dendrites oriented in any direction. It is clear that the maximum field would result from parallel alignment, while other orientations would only diminish this quantity. With that in mind, our first calculations consider the simplified case in which all dipole are oriented in the x-direction to get an upper bound on potential field strengths. We then consider dipoles oriented randomly in the x-y plane.

Equation (5) gives the value of the equivalent current dipole of a dendrite, \mathbf{p} , used during this investigation. Then we use Eq. (3) to calculate the z component of the magnetic field of a dendrite at a given coordinate. During the simulations, dipoles are assigned to locations on a lattice with spacing and orientation depending upon each particular simulation. The contribution to the magnetic field from each dipole is added at each lattice point, producing the resultant field. We assume that the dendrites are active for a time of roughly 10 ms during their depolarization, which is less than the echo time. The magnetic field is treated as effectively constant during the activation time and zero otherwise. With this approximation,

the phase shift ϕ given by Eq. (4) becomes the product of the magnetic field, the gyromagnetic ratio, and the activation time

Furthermore, the field within the voxel will clearly be at a maximum if all the dendrites are active simultaneously. That is, if some of the dendrites are inactive, they certainly will not contribute to the overall field. As such, our first calculations also assume synchronous activation.

Results

Figure 1 depicts the z component of the magnetic field generated by a line of evenly spaced ($10\ \mu\text{m}$) 100 dipoles centered in the voxel. The magnetic field is calculated in the plane containing the dipoles, where it would be largest. This arrangement yielded a maximum magnetic field of 0.049 nT with a corresponding phase shift of 8.3×10^{-5} radians. The magnetic field is large only near the end of the line of dipoles. In the central region, the magnetic fields of the individual dipoles largely cancel. Thus, one can think of the magnetic field as detecting primarily the edge of a region of depolarization.

Figure 2 shows the simulated z component of the magnetic field from a full-voxel simulation of 50,000 dendrites with a uniform spacing of approximately $28\ \mu\text{m}$ in each direction. The maximum field strength is calculated to be 0.44 nT, giving a phase shift of 0.0012 radians, which is slightly less than the minimum detectable limit. The magnetic field is calculated on a plane through the center of the voxel, and again is largest near the voxel edge.

Figure 3 shows the simulated z component of the magnetic field for a full voxel simulation of 10^6 dendrites uniformly arranged in the voxel with a spacing of $10\ \mu\text{m}$ in each direction on the lattice. This simulation corresponds most closely to the accepted physical dendrite density of cortical tissue, and assumes all the dendrites are simultaneously active. In this simulation, the maximum field was found to be 7.76 nT, and the corresponding phase shift was calculated to be 0.021 radians. This simulation resulted in a phase shift that is about an order of magnitude greater than our minimum detectable value. However, for reasons discussed more fully later, this calculated value almost certainly overestimates the phase shift caused by actual cortical dendrites.

For comparison, we also performed a series of simulations with dipoles oriented randomly in the x-y plane. This randomization more closely mirrors the real, physical orientation of the dendrites. At each density, we performed several (5 – 8) simulations with different random orientations and then we averaged the resultant magnetic fields. Our findings are shown in Table 1 together with a comparison to the original, non-randomized orientations. Overall, one notices that as the dendrite density increases, the fraction of the maximum field strength generated by the voxel decreases sharply. At the physically realistic density of 10^6 dendrites per voxel, randomized orientations reduced the maximum z component of the magnetic field in the voxel to roughly 0.22 nT, less than 3% of its original value. Furthermore, Figure 4 shows a representative example of the z component of the magnetic field generated by randomly oriented dendrites. One observes the oscillation in sign of the local maxima and minima, over distances much smaller than a single voxel.

Discussion

The goal of this study is to generate a theoretical model that describes the magnetic field generated by the receptor potentials of dendrites in grey matter, and to assess the feasibility of imaging the related currents via MRI. Overall, our results show that the magnetic fields generated by dendrites may, under the most ideal of circumstances, just barely be detectable

using current MRI techniques. Although 10^6 uniformly oriented, synchronously active dendrites could generate a measurable signal, this situation is unlikely to occur within an actual human brain, except perhaps during an epileptic seizure [24]. In the more physically realistic case of randomly oriented dendrites, we found that the maximum field is sharply reduced and was well below the limit of detectability. The random distribution of dipoles may underestimate the magnetic field, just as the uniform distribution surely overestimates it. More likely is a fairly random distribution at a large spatial scale, but a more uniform distribution over smaller scales. We do not have a good value for the spatial correlation length, so we present the two extreme cases as upper and lower limits. As shown by the other simulations, the field strength and phase shifts also diminish when fewer dendrites are active. During normal brain function, only a small fraction of the dendrites would typically be active simultaneously. Therefore, we are not optimistic about the potential for measuring dendritic activity with current MRI techniques.

As mentioned previously, our results likely overestimate the effects of the dendrites on the MRI signal for several reasons. 1) The magnetic field of a dendrite has both depolarization and repolarization phases as the transmembrane potential rises and falls over time. The repolarization phase has a longer duration than the depolarization phase, but is also weaker, so the integrated biphasic signal is nearly zero, as the phase shifts associated with depolarization and repolarization cancel. The entire dendritic signal may last just a few milliseconds, which is brief relative to MRI imaging pulse sequences. Thus, dendritic signals will be more difficult to detect than we predict, unless fast carefully-timed pulse sequences are developed that detect the phase shift over the depolarization phase but do not cancel out this phase shift during the repolarization phase. 2) The measured signal in a MRI experiment would represent an average over the voxel. The magnetic field distributions in Figs. 1–4 suggest that the average signal may be much less than the maximum signal. 3) The dendrites in the voxel will generally not be active simultaneously. Some may be depolarizing while others are repolarizing. 4) The currents of the brain will generally not point in the same direction. 5) Our simulations probably overestimate the magnetic field because the dipoles are assumed to lie in the x-y plane, whereas in the brain the dipoles may have a z-component that does not contribute to the phase shift because it produces no z-directed magnetic field.

We suspect that the minimum detectable phase shift of 0.1° may be an overestimate. This was measured in experiments using a large voxel size, at least 20 times larger than our voxel [3]. The magnetic field of a wire falls off more slowly than that of a dipole, causing the field to spread over a fairly large area so that a large voxel size should provide a relatively large signal. The phantom used was not a realistic model of living tissue. In a real brain, there could be many sources of noise that are not present in such a phantom experiment. Bodurka and Banditinni mention “physiological noise” which represents magnetic fields produced by any other sources of current (other nerves, muscles in the scalp, the eye, the heart, etc). There is also the impact of time-dependent heterogeneities of the permeability (the source of the BOLD signal), and also movement artifacts due to either breathing or pulsatile blood flow. Finally, any magnetic impurities (magnetite) or contrast agents (gadolinium) could affect our analysis. These factors are difficult to quantify, but all would seem to increase the minimum detectable phase shift arising from neural activation in the brain.

We assume that the magnetic resonance imaging device uses a typical static magnetic field strength on the order of a few Tesla. Neural currents might be detected more easily using ultra-low field MRI [7, 17]. Unlike the chemical shift or susceptibility effects, the biomagnetic field is not proportional to the static magnetic field. Therefore, a lower static field means a larger fractional change in frequency. Ultra-low field systems may be advantageous for these measurements. Perhaps polarizing the spins in a large field and then

reducing it during detection would improve the signal, if the field could be switched rapidly enough.

In conclusion, we find that MRI measurements of neural currents in dendrites may be barely detectable using current technology in extreme cases such as seizures, but the chance of detecting normal brain function is very small. Nevertheless, MRI researchers continue to develop clever new imaging methods, using either sophisticated pulse sequences or data processing. Hopefully, this paper will outline the challenges that must be overcome in order to image dendritic activity using MRI.

Acknowledgments

This research was supported by the National Institutes of Health grant R01EB008421 and the Indiana Academy of Science.

References

1. Bandettini PA, Petridou N, Bodurka J. Direct detection of neuronal activity with MRI: fantasy, possibly, or reality? *Appl Magn Reson*. 2005; 29:65–88.
2. Bandettini PA, Wong EC, Hinks RS, Tikofsky RS, Hyde JS. Time course EPI of human brain function during task activation. *Magn Reson Med*. 1992; 25:390–397. [PubMed: 1614324]
3. Bodurka J, Bandettini PA. Toward direct mapping of neuronal activity: MRI detection of ultraweak transient magnetic field changes. *Magn Reson Med*. 2002; 47:1052–1058. [PubMed: 12111950]
4. Bodurka J, Jesmanowicz A, Hyde JS, Xu H, Estkowski L, Li SJ. Current-induced magnetic resonance phase imaging. *J Mag Res*. 1999; 137:265–271.
5. Callaghan PT. Susceptibility-limited resolution in nuclear magnetic resonance microscopy. *J Magn Reson*. 1990; 87:304–318.
6. Cassara AM, Hagberg GE, Bianciardi M, Migliore M, Maraviglia B. Realistic simulations of neuronal activity: A contribution to the debate on direct detection of neuronal currents by MRI. *NeuroImage*. 2008; 39:87–106. [PubMed: 17936018]
7. Cassara AM, Maraviglia B. Microscopic investigation of the resonant mechanism for the implementation of nc-MRI at ultra-low field MRI. *NeuroImage*. 2008; 41:1228–1241. [PubMed: 18474435]
8. Chu R, de Zwart J, van Gelderen P, Fukunaga M, Kellman P, Holroyd T, Duyn JH. Hunting for neuronal currents: absence of rapid MRI signal changes during visual-evoked response. *Neuroimage*. 2004; 23:1059–1067. [PubMed: 15528106]
9. Gielen FLH, Roth BJ, Wikswo JP. Capabilities of a toroid-amplifier system for magnetic measurement of current in biological tissue. *IEEE Trans Biomed Eng*. 1986; 33:910–921. [PubMed: 3770779]
10. Gielen FLH, Friedman RN, Wikswo JP. In vivo magnetic and electric recordings from nerve bundles and single motor units in mammalian skeletal muscle. *J Gen Physiol*. 1991; 98:1043–1061. [PubMed: 1765761]
11. Hagberg GE, Bianciardi M, Maraviglia B. Challenges for detection of neuronal currents by MRI. *Magn Reson Med*. 2006; 24:483–493.
12. Hennig J, Zhong K, Speck O. MR-encephalography: fast multi-channel monitoring of brain physiology with magnetic resonance. *NeuroImage*. 2008; 39:310–317. [PubMed: 17920296]
13. Johnston D, Magee JC, Colbert CM, Christie BR. Active properties of neuronal dendrites. *Annu Rev Neurosci*. 1996; 19:165–186. [PubMed: 8833440]
14. Kamei H, Iramina K, Yoshikawa K, Ueno S. Neuronal current distribution imaging using magnetic resonance. *IEEE Trans Magn*. 1999; 35:4109–4111.
15. Kaufman L, Kaufman JH, Wang J-Z. On cortical folds and neuromagnetic fields. *Electroenceph Clin Neurophys*. 1991; 79:211–229.

16. Konn D, Gowland P, Bowtell R. MRI detection of weak magnetic fields due to an extended current dipole in a conduction sphere: A model for direct detection of neuronal currents in the brain. *Magn Reson Med.* 2003; 50:40–49. [PubMed: 12815677]
17. Kraus RH, Volegov P, Matlachov A, Espy M. Toward direct neural current imaging by resonant mechanisms at ultra-low field. *Neuroimage.* 2008; 39:310–317. [PubMed: 17920296]
18. Kwong K, Brady T, Rosen B. Dynamic magnetic resonance imaging of human brain activity during primary sensory stimulation. *Proc Natl Acad Sci USA.* 1992; 89:5675–5679. [PubMed: 1608978]
19. Nunez, PL.; Srinivasan, R. *Electric Fields of the Brain the Neurophysics of EEG.* 2nd ed.. Oxford University Press; New York: 2006.
20. Ogawa S, Lee TM, Kay AR, Tank DW. Brain magnetic resonance imaging with contrast dependence on blood oxygenation. *Proc Natl Acad Sci USA.* 1990; 87:9868–9872. [PubMed: 2124706]
21. Paley MNJ, Chow LS, Whitby EW, Cook GG. Modelling of axonal fields in the optic nerve for direct MR detection studies. *Imag Vision Comput.* 2009; 27:331–341.
22. Park TS, Lee SY. Effects of neuronal magnetic field on MRI: Numerical analysis with axon and dendrite models. *NeuroImage.* 2007; 35:531–538. [PubMed: 17291782]
23. Roth BJ, Wikswo JP. The magnetic field of a single nerve axon: A comparison of theory and experiment. *Biophys J.* 1985; 48:93–109. [PubMed: 4016213]
24. Sundaram P, Wells WM, Mulkern RV, Bublick EJ, Bromfield EB, Munch M, Orbach DB. Fast human brain magnetic resonance responses associated with epileptiform spikes. *Magn Reson Med.* 2010; 64:1728–1738. [PubMed: 20806355]
25. Swinney KR, Wikswo JP. A calculation of the magnetic field of a nerve action potential. *Biophys J.* 1980; 32:719–732. [PubMed: 7260298]
26. Truong TK, Song AW. Finding neuroelectric activity under magnetic field oscillations (NAMO) with magnetic resonance imaging in vivo. *Proc. Natl. Acad. Sci. USA.* 2006; 103:12598–12601. [PubMed: 16894177]
27. van Egeraat JM, Friedman RN, Wikswo JP. Magnetic field of a single muscle fiber: First measurement and a core conductor model. *Biophys J.* 1990; 57:663–667. [PubMed: 2306511]
28. van Egeraat JM, Wikswo JP. A model for axonal propagation incorporating both radial and axial ionic transport. *Biophys J.* 1993; 64:1287–1298. [PubMed: 8388269]
29. van Egeraat JM, Stasaski R, Barach JP, Friedman RN, Wikswo JP. The biomagnetic signature of a crushed axon: A comparison of theory and experiment. *Biophys J.* 1993; 64:1299–1305. [PubMed: 8494985]
30. Wijesinghe RS, Gielen FLH, Wikswo JP. A model for compound action potentials and currents in a nerve bundle III: A comparison of the conduction velocity distributions calculated from compound action currents and potentials. *Ann Biomed Eng.* 1991; 18:97–121. [PubMed: 2035912]
31. Wijesinghe RS, Roth BJ. Detection of Peripheral Nerve and Skeletal Muscle Action Currents Using Magnetic Resonance Imaging. *Ann Biomed Eng.* 2009; 37(11):2402–2406. [PubMed: 19609834]
32. Wikswo JP, van Egeraat JM. Cellular magnetic fields: Fundamental and applied measurements on nerve axons, peripheral nerve bundles, and skeletal muscle. *J Clin Neurophysiol.* 1991; 8:170–188. [PubMed: 2050817]
33. Wikswo JP, Barach JP, Freeman JA. Magnetic field of a nerve impulse: First measurements. *Science.* 1980; 208:53–55. [PubMed: 7361105]
34. Wikswo, JP.; Henry, WP.; Freidman, RN.; Kilroy, WA.; Wijesinghe, RS.; van Egeraat, JM.; Milek, MA. Intraoperative recording of the magnetic field of a human nerve. In: Williamson, SJ.; Hoke, M.; Stroink, G.; Kotani, M., editors. *Advances in Biomagnetism.* Plenum; New York: 1990. p. 137-140.
35. Woosley JK, Roth BJ, Wikswo JP. The magnetic field of a single axon: A volume conductor model. *Math Biosci.* 1985; 76:1–36.
36. Xue X, Chen X, Grabowski T, Xiong J. Direct MRI mapping of neuronal activity evoked by electrical stimulation of the median nerve at the right wrist. *Magn Reson Med.* 2009; 61:1073–1082. [PubMed: 19466755]

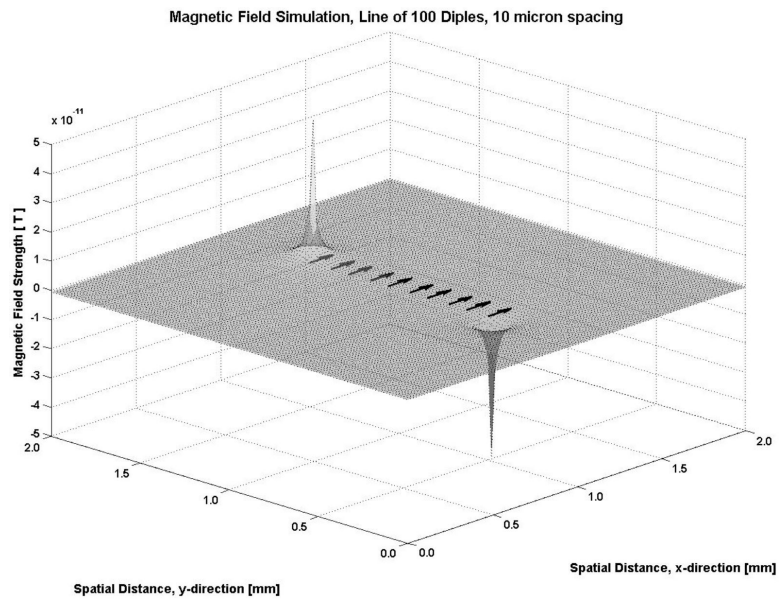


Fig. 1. The field from a line of 100 dipoles positioned uniformly across a 1 mm line with a spacing of 10 μm . A sampling value of 10 μm was used to generate the plot. Arrows indicate the general locations and directions of the dipoles in the simulation.

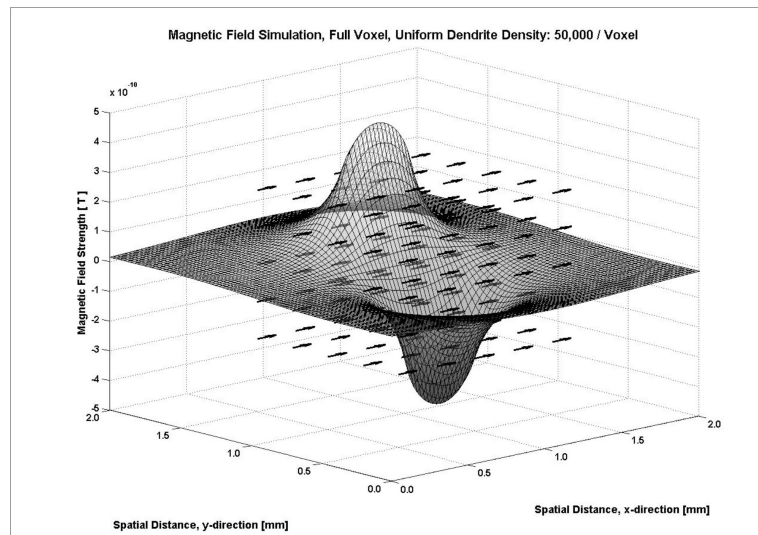


Fig. 2. The magnetic field from a full voxel containing 50,000 dipoles. The dipoles were arranged uniformly with an approximate spacing $28 \mu\text{m}$ in each direction, and a sampling value of $20 \mu\text{m}$ was used to generate this plot. Arrows indicate the general locations and directions of the dipoles in the simulation.

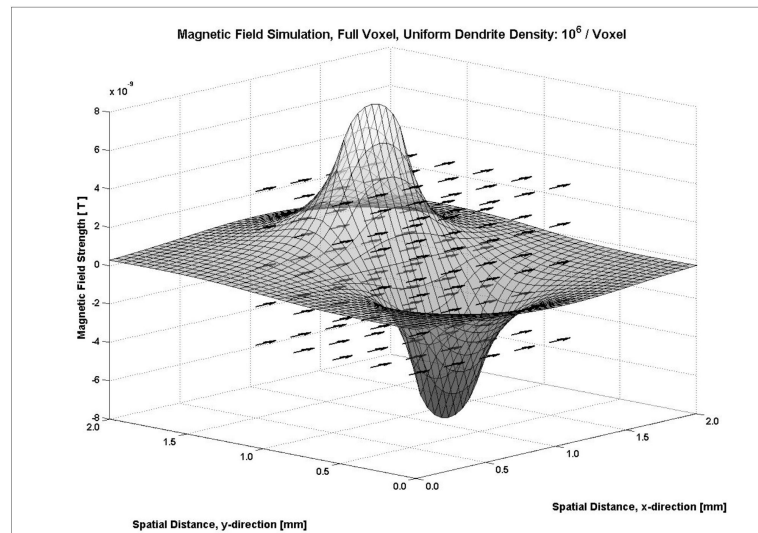


Fig. 3. The magnetic field from a full voxel containing 10^6 dipoles. The dipoles were arranged uniformly with a spacing of $10\ \mu\text{m}$ in each direction, and a sampling value of $50\ \mu\text{m}$ was used to generate this plot. Arrows indicate the general locations and directions of the dipoles in the simulation

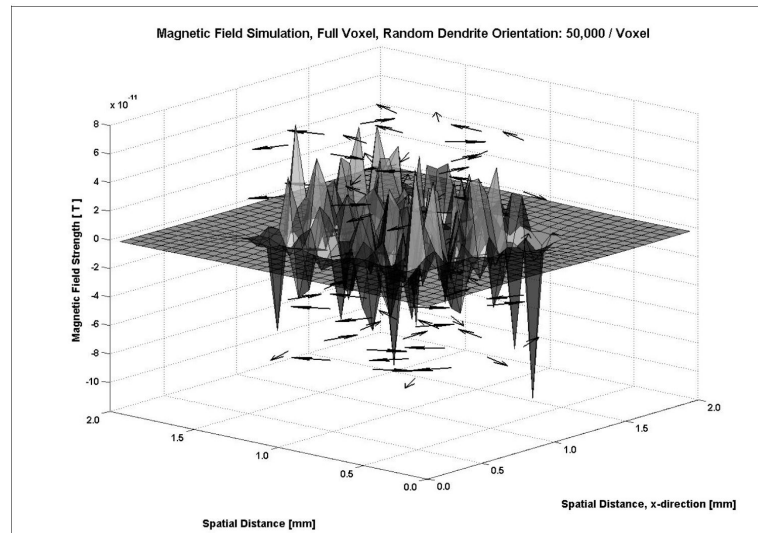


Fig. 4. The magnetic field from a full voxel containing 50,000 dipoles, each with a random orientation. The dipoles were arranged with uniform spacing of approximately $28 \mu\text{m}$ in each direction, and a sampling value of $70 \mu\text{m}$ was used to generate this plot. Arrows indicate the general locations and directions of the dipoles in the simulation.

Table 1

Summary and Comparison of Representative Simulation Results

	Dendrite Density (dipoles / mm ³)	Uniformly Orientation		Random Orientation	
		Maximum B-Field (nT)	Phase Shift (radians)	Average Maximum B-Field (nT)	Percent of Non-Random Orientation
Layer	10,000	0.14	0.00038	0.09	65%
Full Voxel	50,000	0.44	0.0012	0.13	30%
Full Voxel	100,000	0.87	0.0023	0.16	18%
Full Voxel	1,000,000	7.76	0.021	0.22	2.6%

NOTE: The proposed detection threshold was 0.0017 radians.